Supplementary Materials for "Altermagnetism and Strain Induced Altermagnetic Transition in Cairo Pentagonal Monolayer"

Shuyi Li,[1] Yu Zhang,[1] Adrian Bahri,[1] Xiaoliang Zhang,[1] and Chunjing Jia[1]

[1]*Department of Physics, University of Florida, Gainesville, FL 32611, USA*

I. TIGHT-BINDING MODEL

The Cairo pentagonal lattice under consideration is shown in Fig. I. The lattice vectors are defined as $\mathbf{a}_1 = (a, 0)$ and $\mathbf{a}_2 = (0, a)$, where a is the lattice constant and set to be 1 for convenience. Each primitive unit cell contains two magnetic sites and four non-magnetic sites, their coordinates are

$$\begin{aligned} \text{magnetic}: &(0,0),\ (\frac{a}{2},\frac{a}{2}) \\ \text{non-magnetic}: &(d,\frac{a}{2}-d),\ (d-\frac{a}{2},d),\ (-d,d-\frac{a}{2}),\ (\frac{a}{2}-d,-d), \end{aligned} \tag{S1}$$

where $0 < d < a/2$. Without loss of generality, we set spin-up site at $(0, 0)$, and $0 < d = 0.1a < a/4$ in our calculation.

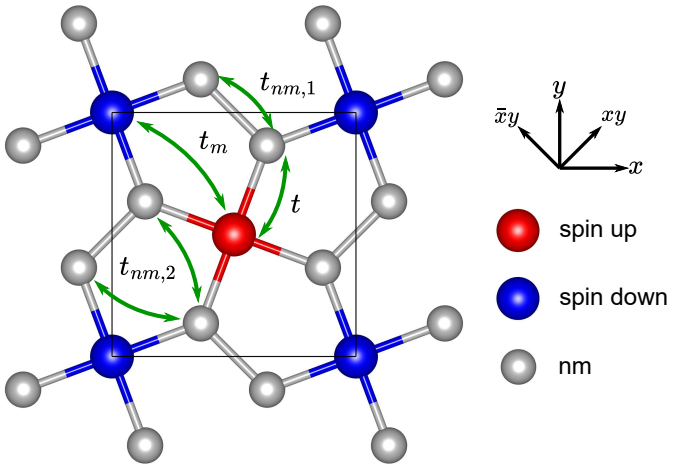

FIG. S1. A schematic of the pentagonal lattice with space group $P4/mbm$ and the tight-binding model on it.

The tight-binding Hamiltonian is

$$\begin{aligned} H = &-(1+\delta)\sum_{\langle i,j\rangle_{xy}} t_{ij}c^\dagger_{i\sigma}c_{j\sigma} - (1-\delta)\sum_{\langle i,j\rangle_{\bar{x}y}} t_{ij}c^\dagger_{i\sigma}c_{j\sigma} - J\sum_{i\in \mathrm{m},\sigma,\sigma'} \mathbf{S}_i \cdot c^\dagger_{i\sigma}\boldsymbol{\sigma}_{\sigma\sigma'}c_{i\sigma'} \\ &+ (\epsilon_m - \mu)\sum_{i\in m,\sigma} c^\dagger_{i\sigma}c_{i\sigma} + (\epsilon_{nm} - \mu)\sum_{i\in nm,\sigma} c^\dagger_{i\sigma}c_{i\sigma}, \end{aligned} \tag{S2}$$

where δ represents the strength of anisotropy caused by diagonal strains. We perform Fourier transformation into each electron operator

$$c_{i\sigma} = \frac{1}{\sqrt{N}}\sum_{\mathbf{k}} c_{\mathbf{k}\sigma}e^{i\mathbf{r}_i\mathbf{k}} \tag{S3}$$

, where N is the number of unit cells. Then the Hamiltonian in Eq. (S2) becomes

$$H = \sum_{\mathbf{k},\sigma} \psi^\dagger_{\mathbf{k}\sigma} H_{\mathbf{k}\sigma}\psi_{\mathbf{k}\sigma}, \tag{S4}$$

where $\psi^{\dagger}_{\mathbf{k}\sigma} = [c^{\dagger}_{1\sigma\mathbf{k}}, \cdots, c^{\dagger}_{6\sigma\mathbf{k}}]$. The matrices $H_{\mathbf{k}\sigma}$ are written as

$$H_{\mathbf{k}\uparrow} = \begin{bmatrix} \epsilon_m - JS & t_{AB} & t_{A\alpha} & t_{A\beta} & t_{A\gamma} & t_{A\eta} \\ t^*_{AB} & \epsilon_m + JS & t_{B\alpha} & t_{B\beta} & t_{B\gamma} & t_{B\eta} \\ t^*_{A\alpha} & t^*_{B\alpha} & \epsilon_{nm} & t_{\alpha\beta} & t_{\alpha\gamma} & t_{\alpha\eta} \\ t^*_{A\beta} & t^*_{B\beta} & t^*_{\alpha\beta} & \epsilon_{nm} & t_{\beta\gamma} & t_{\beta\eta} \\ t^*_{A\gamma} & t^*_{B\gamma} & t^*_{\alpha\gamma} & t^*_{\beta\gamma} & \epsilon_{nm} & t_{\gamma\eta} \\ t^*_{A\eta} & t^*_{B\eta} & t^*_{\alpha\eta} & t^*_{\beta\eta} & t^*_{\gamma\eta} & \epsilon_{nm} \end{bmatrix} - \mu * \mathbb{1}_{6\times 6}, \tag{S5}$$

and

$$H_{\mathbf{k}\downarrow} = \begin{bmatrix} \epsilon_m + JS & t_{AB} & t_{A\alpha} & t_{A\beta} & t_{A\gamma} & t_{A\eta} \\ t^*_{AB} & \epsilon_m - JS & t_{B\alpha} & t_{B\beta} & t_{B\gamma} & t_{B\eta} \\ t^*_{A\alpha} & t^*_{B\alpha} & \epsilon_{nm} & t_{\alpha\beta} & t_{\alpha\gamma} & t_{\alpha\eta} \\ t^*_{A\beta} & t^*_{B\beta} & t^*_{\alpha\beta} & \epsilon_{nm} & t_{\beta\gamma} & t_{\beta\eta} \\ t^*_{A\gamma} & t^*_{B\gamma} & t^*_{\alpha\gamma} & t^*_{\beta\gamma} & \epsilon_{nm} & t_{\gamma\eta} \\ t^*_{A\eta} & t^*_{B\eta} & t^*_{\alpha\eta} & t^*_{\beta\eta} & t^*_{\gamma\eta} & \epsilon_{nm} \end{bmatrix} - \mu * \mathbb{1}_{6\times 6}, \tag{S6}$$

where the matrix elements are

$$\begin{aligned}
t_{AB} &= -2t_m(1+\delta)\cos\Big(\frac{a}{2}k_x + \frac{a}{2}k_y\Big) - 2t_m(1-\delta)\cos\Big(\frac{a}{2}k_x - \frac{a}{2}k_y\Big), \\
t_{A\alpha} &= -t(1-\delta)e^{i((\frac{a}{2}-d)k_x - dk_y)}, \\
t_{A\beta} &= -t(1-\delta)e^{i(-(\frac{a}{2}-d)k_x + dk_y)}, \\
t_{A\gamma} &= -t(1+\delta)e^{i(dk_x + (\frac{a}{2}-d)k_y)}, \\
t_{A\eta} &= -t(1+\delta)e^{i(-dk_x - (\frac{a}{2}-d)k_y)}, \\
t_{B\alpha} &= -t(1-\delta)e^{i(-dk_x + (-d+\frac{a}{2})k_y)}, \\
t_{B\beta} &= -t(1-\delta)e^{i(dk_x + (d-\frac{a}{2})k_y)}, \\
t_{B\gamma} &= -t(1+\delta)e^{i((d-\frac{a}{2})k_x - dk_y)}, \\
t_{B\eta} &= -t(1+\delta)e^{i((-d+\frac{a}{2})k_x + dk_y)}, \\
t_{\alpha\beta} &= -t_{nm,1}(1+\delta)e^{i(2dk_x + 2dk_y)}, \\
t_{\alpha\gamma} &= -t_{nm,2}(1+\delta)e^{i((2d-\frac{a}{2})k_x - \frac{a}{2}k_y)} - t_{nm,2}(1-\delta)e^{i((2d-\frac{a}{2})k_x + \frac{a}{2}k_y)}, \\
t_{\alpha\eta} &= -t_{nm,2}(1+\delta)e^{i(-\frac{a}{2}k_x + (2d-\frac{a}{2})k_y)} - t_{nm,2}(1-\delta)e^{i(\frac{a}{2}k_x + (2d-\frac{a}{2})k_y)}, \\
t_{\beta\gamma} &= -t_{nm,2}(1+\delta)e^{i(\frac{a}{2}k_x + (\frac{a}{2}-2d)k_y)} - t_{nm,2}(1-\delta)e^{i(-\frac{a}{2}k_x + (\frac{a}{2}-2d)k_y)}, \\
t_{\beta\eta} &= -t_{nm,2}(1+\delta)e^{i((\frac{a}{2}-2d)k_x + \frac{a}{2}k_y)} - t_{nm,2}(1-\delta)e^{i((\frac{a}{2}-2d)k_x - \frac{a}{2}k_y)}, \\
t_{\gamma\eta} &= -t_{nm,1}(1-\delta)e^{i(-2dk_x + 2dk_y)},
\end{aligned} \tag{S7}$$

and $\mathbb{1}_{6\times 6}$ is a 6×6 identity matrix.

II. TAYLOR EXPANSION OF $E_{n,\sigma}(\mathbf{k})$ NEAR Γ POINT

We investigate the behavior of band dispersions near Γ point by performing Taylor expansion. Near $\mathbf{k} = \mathbf{0}$, we assume that an isolated band can be represented by

$$\begin{aligned}
E_\sigma(\mathbf{k}) = a_{0,\sigma} &+ a_{21,\sigma}k_x^2 + a_{22,\sigma}k_xk_y + a_{23,\sigma}k_y^2 \\
&+ a_{41,\sigma}k_x^4 + a_{42,\sigma}k_x^3k_y + a_{43,\sigma}k_x^2k_y^2 + a_{44,\sigma}k_xk_y^3 + a_{45,\sigma}k_y^4,
\end{aligned} \tag{S8}$$

there is no linear and cubic term because of inversion symmetry. Then we expand the characteristic equation

$$\det|E_\sigma \mathbb{1}_{6\times 6} - H_{\mathbf{k}\sigma}| = 0 \tag{S9}$$

at $\mathbf{k} = \mathbf{0}$ to solve the coefficients.

The model parameters used are $t_m = -0.4$, $t_{nm,1} = 0.9$, $t_{nm,2} = 0.6$, $J = 1$, $\epsilon_m = \epsilon_{nm} = 0$ and $\mu = 0$. In the case of $\delta = 0$, there are four isolated bands near the Γ point for each spin, the coefficients are in Table. I. The leading term of spin-splitting for the nth pair bands near the Γ point is

$$\Delta E_n(\mathbf{k}) = 2a_{n,42,\uparrow}k_xk_y(k_x^2 - k_y^2), \tag{S10}$$

which is belong to g-wave symmetry.

Band Index n	1	2	5	6
$a_{0,\uparrow}$	-5.19	0.106	1.5	1.79
$a_{21,\uparrow}$	0.267	-0.414	0.3	0.27
$a_{22,\uparrow}$	0	0	0	0
$a_{23,\uparrow}$	0.267	-0.414	0.3	0.27
$a_{41,\uparrow}$	-0.00425	-0.0341	-0.664	0.0497
$a_{42,\uparrow}$	0.000141	-0.166	1.35	-0.491
$a_{43,\uparrow}$	-0.0111	0.631	-0.551	-0.00221
$a_{44,\uparrow}$	-0.000141	0.166	-1.35	0.491
$a_{45,\uparrow}$	-0.00425	-0.0341	-0.664	0.0497
$a_{0,\downarrow}$	-5.19	0.106	1.5	1.79
$a_{21,\downarrow}$	0.267	-0.414	0.3	0.27
$a_{22,\downarrow}$	0	0	0	0
$a_{23,\downarrow}$	0.267	-0.414	0.3	0.27
$a_{41,\downarrow}$	-0.00425	-0.0341	-0.664	0.0497
$a_{42,\downarrow}$	-0.000141	0.166	-1.35	0.491
$a_{43,\downarrow}$	-0.0111	0.631	-0.551	-0.00221
$a_{44,\downarrow}$	0.000141	-0.166	1.35	-0.491
$a_{45,\downarrow}$	-0.00425	-0.0341	-0.664	0.0497

TABLE I. Coefficients of $E_{n,\sigma}(\mathbf{k})$ in the case of $\delta = 0$.

Band Index n	1	2	3	4	5	6
$a_{0,\uparrow}$	-0.519	0.0821	0.81	0.99	1.4	1.91
$a_{21,\uparrow}$	0.266	-0.416	-0.228	-0.0392	0.0625	0.355
$a_{22,\uparrow}$	0.0401	-0.203	0.432	-0.804	0.756	-0.221
$a_{23,\uparrow}$	0.268	-0.392	-0.0054	-0.894	1.01	0.0129
$a_{0,\downarrow}$	-0.519	0.0821	0.81	0.99	1.4	1.91
$a_{21,\downarrow}$	0.268	-0.392	-0.0054	-0.894	1.01	0.0129
$a_{22,\downarrow}$	0.0401	-0.203	0.432	-0.804	0.756	-0.221
$a_{23,\downarrow}$	0.266	-0.416	-0.228	-0.0392	0.0625	0.355

TABLE II. Coefficients of $E_{n,\sigma}(\mathbf{k})$ in the case of $\delta = 0.1$.

In the case of $\delta = 0.1$, there are six isolated bands near the Γ point for each spin, the coefficients are in Table. II. The leading term of spin-splitting for the nth pair bands near the Γ point is

$$\Delta E_n(\mathbf{k}) = (a_{n,21,\uparrow} - a_{n,23,\uparrow})(k_x^2 - k_y^2), \tag{S11}$$

which is belong to d-wave symmetry.

III. BAND DEGENERACY UNDER $t_{nm,1} = 0$ AND $t_{nm,2} = 0$

The case of $t_{nm,1} = 0$ is equivalent to that of a lattice with $d = a/4$, which is shown in Fig. S2. This system clearly exhibits mirror symmetries $\mathcal{M}_x$ and $\mathcal{M}_y$.

The case of $t_{nm,2} = 0$ is equivalent to that of a lattice with $d = 0$. With this formula, it can be directly shown that the characteristic equations of $H_{kx,ky,\sigma}$, $H_{kx,-ky,\sigma}$, and $H_{-kx,ky,\sigma}$ are the same:

$$\begin{aligned} \det|E\mathbb{1}_{6\times6} - H_{kx,ky,\sigma}| &= \det|E\mathbb{1}_{6\times6} - H_{kx,-ky,\sigma}|, \\ \det|E\mathbb{1}_{6\times6} - H_{kx,ky,\sigma}| &= \det|E\mathbb{1}_{6\times6} - H_{-kx,ky,\sigma}|, \end{aligned} \tag{S12}$$

which implies that $E_{n,\sigma}(kx, ky) = E_{n,\sigma}(kx, -ky) = E_{n,\sigma}(-kx, ky)$. The combination of these symmetries with $\{C_{2\perp}||\mathcal{M}_x\}$ and $\{C_{2\perp}||\mathcal{M}_y\}$ ensures that $E_{n,\uparrow}(\mathbf{k}) = E_{n,\downarrow}(\mathbf{k})$.

IV. BERRY CURVATURE

After taking into account the symmetry breaking terms

$$H_1 = \sum_{i\in(m\uparrow),\sigma} \sum_{\boldsymbol{\xi}} (t_1 c^\dagger_{i,\sigma} c_{i+\boldsymbol{\xi}\sigma} - t_1 c^\dagger_{i\sigma} c_{i-\boldsymbol{\xi},\sigma}) + h.c. \tag{S13}$$

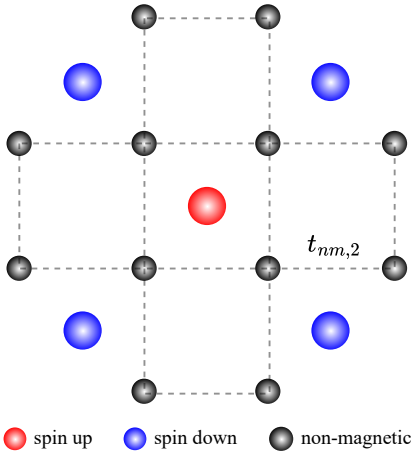

FIG. S2. The equivalent lattice of the Cairo pentagonal lattice when $t_{nm,1} = 0$ in its tight-binding model.

and

$$H_2 = -\sum_{i\in(m\uparrow),\sigma}(-1)^{\sigma}\sum_{\boldsymbol{\xi}} i(t_2 c^{\dagger}_{i,\sigma}c_{i+\boldsymbol{\xi}\sigma} + t_2 c^{\dagger}_{i\sigma}c_{i-\boldsymbol{\xi},\sigma}) + h.c., \tag{S14}$$

we perform the same process as in Eq.(S3) and Eq.(S4) to obtain the Hamiltonian matrix $H^{total}_{\mathbf{k}\sigma}$. Then we use Fukui's method to calculate Berry curvature $\Omega_{n,\sigma}(\mathbf{k})$ and Chern number $\mathcal{C}_{n,\sigma}$ numerically [S1], which is given by

$$\begin{aligned}
&\Omega_{n,\sigma}(k_x + \frac{1}{2}\delta k_x, k_y + \frac{1}{2}\delta k_y)\\
=&-\frac{1}{\delta k_x \delta k_y}\mathrm{Arg}[\langle u_{n,\sigma}(k_x,k_y)|u_{n,\sigma}(k_x+\frac{1}{2}\delta k_x,k_y)\rangle\\
&\langle u_{n,\sigma}(k_x+\frac{1}{2}\delta k_x,k_y)|u_{n,\sigma}(k_x+\frac{1}{2}\delta k_x,k_y+\frac{1}{2}\delta k_y)\rangle\\
&\langle u_{n,\sigma}(k_x+\frac{1}{2}\delta k_x,k_y+\frac{1}{2}\delta k_y)|u_{n,\sigma}(k_x,k_y+\frac{1}{2}\delta k_y)\rangle\\
&\langle u_{n,\sigma}(k_x,k_y+\frac{1}{2}\delta k_y)|u_{n,\sigma}(k_x,k_y)\rangle],
\end{aligned} \tag{S15}$$

$$\mathcal{C}_{n,\sigma} = \frac{1}{2\pi}\sum_{\mathbf{k}}\Omega_{n,\sigma}(k_x+\frac{1}{2}\delta k_x, k_y+\frac{1}{2}\delta k_y)\delta k_x \delta k_y, \tag{S16}$$

where $|u_{n,\sigma}(k_x,k_y)\rangle$ is the nth eigenvector of the Hamiltonian $H^{total}_{\mathbf{k}\sigma}$. In the summation, we choose $\delta k_x = \delta k_y = 2\pi/N_s$ with $N_s = 201$.

V. DETAILS OF *AB INITIO* CALCULATIONS

We use the Vienna Ab initio Simulation Package (VASP) [S2] for all density-functional theory calculations. Projector-augmented-wave (PAW) potentials [S3] were utilized for ion-electron interactions, and the generalized gradient approximation (GGA) with the Perdew-Burke-Ernzerhof (PBE) functional [S4] was applied to describe electron exchange-correlation interactions. The energy cutoff was set to 600 eV.

In the calculation of FeS_2, a $15 \times 15 \times 1$ Monkhorst-Pack k point mesh was used and the GGA + U approach was adopted with $U_{eff} = 2.0$ eV [S5]. The monolayer FeS_2 is exfoliated from the bulk crystal in the (100) plane, forming a planar structure by manually relocating the S atoms. In our calculations, spin-orbit coupling is not included, resulting in the absence of magnetic anisotropy. To determine the magnetic ground state, we relaxed the structure under the ferromagnetic (FM) and Néel antiferromagnetic (AFM) configurations with 0.015 eV/Å and 10^{-6} eV as the convergence criterion for residual force and total-energy, respectively:

$$E_{FM} = -29.138344 \text{ eV}, \ E_{AFM} = -30.641527 \text{ eV}. \tag{S17}$$

The results suggest that the Néel antiferromagnetic configuration has a lower energy with ΔE = -1.50 eV. Keeping the lengths of lattice vectors unchanged, we apply shear strain in the diagonal direction by changing the angle γ between lattice vectors **a** and **b** from 90°to 88°and relax the atomic positions.

For Nb_2FeB_2, a $8 \times 8 \times 13$ Monkhorst-Pack k-point mesh was used, and $U_{eff} = 4.82$ eV [S6] was set for strongly correlated Fe 3d electrons. We relax both lattice constant and atomic positions until the atomic force is less than

0.01eV/Å.

[S1] T. Fukui, Y. Hatsugai, and H. Suzuki, Chern numbers in discretized brillouin zone: efficient method of computing (spin) hall conductances, Journal of the Physical Society of Japan **74**, 1674 (2005).
[S2] G. Kresse and J. Hafner, Ab initio molecular-dynamics simulation of the liquid-metal–amorphous-semiconductor transition in germanium, Phys. Rev. B **49**, 14251 (1994).
[S3] P. E. Blöchl, Projector augmented-wave method, Phys. Rev. B **50**, 17953 (1994).
[S4] J. P. Perdew, K. Burke, and M. Ernzerhof, Generalized gradient approximation made simple, Phys. Rev. Lett. **77**, 3865 (1996).
[S5] A. B. Puthirath, A. P. Balan, E. F. Oliveira, V. Sreepal, F. C. Robles Hernandez, G. Gao, N. Chakingal, L. M. Sassi, P. Thibeorchews, G. Costin, R. Vajtai, D. S. Galvao, R. R. Nair, and P. M. Ajayan, Apparent ferromagnetism in exfoliated ultrathin pyrite sheets, The Journal of Physical Chemistry C **125**, 18927 (2021).
[S6] Z.-F. Gao, S. Qu, B. Zeng, Y. Liu, J.-R. Wen, H. Sun, P.-J. Guo, and Z.-Y. Lu, Ai-accelerated discovery of altermagnetic materials, arXiv preprint arXiv:2311.04418 (2023).